

pubs.acs.org/cm Article

# Enhancement of Photostability through Side Chain Tuning in Dioxythiophene-Based Conjugated Polymers

D. Eric Shen,\* Augustus W. Lang, Graham S. Collier, Anna M. Österholm, Evan M. Smith, Aimée L. Tomlinson, and John R. Reynolds\*



Cite This: Chem. Mater. 2022, 34, 1041-1051



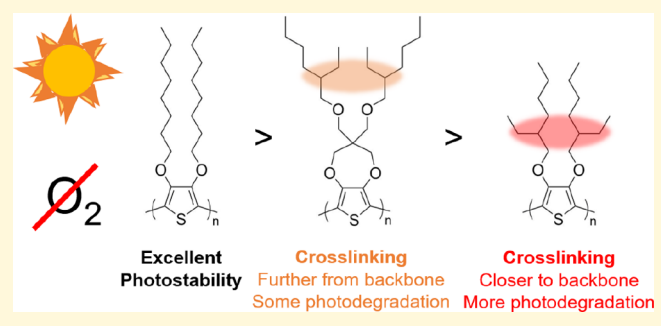
**ACCESS** I

Metrics & More

Article Recommendations

Supporting Information

ABSTRACT: Even as strategies for encapsulating organic electronic devices have become more sophisticated and accessible, resulting in impressive and encouraging long-term stabilities being reported, photodegradation of conjugated polymers continues to occur even under oxygen- and moisture-free conditions. To further enhance the photostability of conjugated materials, it is important to understand fundamental and system-independent photodegradation pathways and the structure—property relationships impacting photostability. As a means to address this, we measure the photostability of thin films under oxygen-free conditions of a family of dialkoxy-functionalized thiophene polymers and evaluate



potential degradation pathways. This approach is enabled by varying the nature and placement of solubilizing groups to pinpoint structural elements and motifs that are particularly susceptible to irreversible photodegradation. Using a combination of UV—vis—NIR spectroscopy, X-ray photoelectron spectroscopy, size exclusion chromatography, nuclear magnetic resonance, and cyclic voltammetry, we evaluate if and how defects such as crosslinking, chain scission, and/or chemical changes affecting the conjugated backbone impact the rate of photodegradation and how they are affected by the placement, design, and branching point of the side chains. We are able to demonstrate that crosslinking through the alkyl side chains is the main degradation pathway under oxygen-free conditions, and that backbone twisting plays an important role in the rate of photodegradation. Based on these findings, we propose that moving away from tertiary carbon branched side chains toward either quaternary carbon branches or linear chains, and/or moving the branching point further from the conjugated backbone, are all promising and relatively straightforward strategies for enhancing photostability in conjugated polymers.

#### ■ INTRODUCTION

In considering the practical use of conjugated polymers in organic electronic devices, one critical property that impacts many figures-of-merit is their photostability. Most conjugated materials undergo rapid photodegradation and complete loss in performance within days under ambient light exposure as a result of both oxidation and hydrolysis. This limits their potential application to devices fully encapsulated under an inert atmosphere, which can be expensive, restrictive, and still prone to degradation, or to disposable and single-use electronic devices with a shorter shelf-life, which prevents their adoption in areas where industrial standards demand years of stability (e.g., architectural windows, environmental sensors, and solar panels). Compared with the large body of work on structure property relationships impacting many practical figures-ofmerit (power conversion efficiency, electrochromic contrast, charge mobility, and capacitance, to name a few), there are relatively few studies on the specific structure-property relationships that directly impact photostability. Being able to pinpoint specific design motifs or structural elements that are particularly susceptible to irreversible photodegradation will allow the field to more rapidly remove these weak links and incorporate conjugated polymers into real-world device platforms through simple structural changes.

To date, the majority of photodegradation studies on conjugated polymers are performed in the presence of oxygen to probe photooxidation, whereas photodegradation studies in the absence of oxygen and moisture remain relatively few. <sup>1–5</sup> The main areas of focus have been on investigating the chemical changes occurring upon photooxidation, the impact of photodegradation on photophysical and material properties, the role that processing and morphology have on photooxidative degradation, the role of triplet vs singlet oxygen, and the impact of quenchers and antioxidants as additives. Most notably, it has been shown that photodegradation, with and

Received: September 25, 2021 Revised: January 4, 2022 Published: January 19, 2022





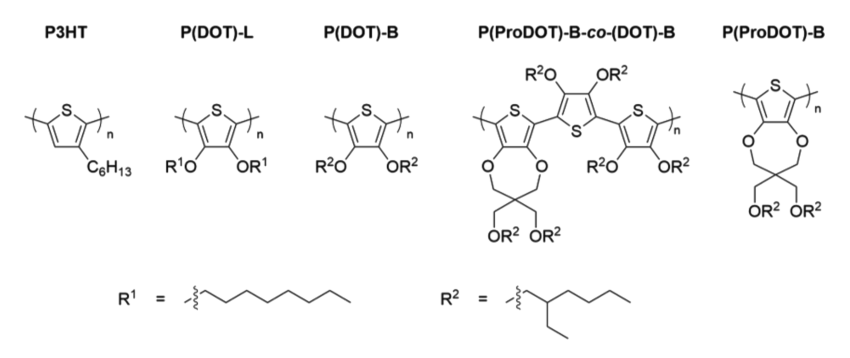


Figure 1. Repeat unit structures of evaluated polymers; B stands for the branched side chain, while the L stands for the linear side chain.

without oxygen present, can be initiated both along the solubilizing side chains and along the conjugated backbone itself.<sup>6,7</sup> However, it has also become clear that many degradation mechanisms are system-dependent, and also dependent on whether solutions or thin films are being evaluated, especially when it comes to how oxygen interacts with the polymer. For example, the role of singlet oxygen<sup>8–10</sup> has been debated, with reports showing both its active role in the degradation process (such as photobleaching via a Diels-Alder reaction with thiophene) 6,8,11 as well as arguments against singlet oxygen's involvement.<sup>3,12</sup> The current consensus is that while singlet oxygen may play a large role in solution photodegradation, it is not a major contributor to thin film photooxidation in systems with low triplet quantum yields, which leads to the formation of singlet oxygen.<sup>8,9</sup> Related to this, the effects of additives such as singlet oxygen quenchers, triplet quenchers, antioxidants, "light screens", 13 and fullerenes<sup>2,14</sup> have been explored and shown to improve shortterm photostability, though this often requires using large amounts of additives (>10%). For applications where oxygen cannot be completely excluded, it is necessary to study the fundamental photophysical properties as characteristics unique to each polymer, which will then dictate the role that singlet oxygen plays in the degradation process. It has also been suggested that the degree of crystallinity in a film may play a role in determining a material's photooxidative stability.A screening of conjugated polymers, oligomers, and small molecules used in organic photovoltaics found a correlation between enhanced photostability with higher degrees of crystallinity and film density, where the authors postulated that crystalline domains can inhibit diffusion of gases and other reactants.<sup>17</sup> However, there is also contradictory evidence from annealing and reaction kinetic studies suggesting that the degree of crystallinity and differences in oxygen diffusion rates alone cannot account for enhanced photostability.<sup>3</sup> While questions about how oxygen interacts with conjugated materials are important, as strategies for encapsulating materials and devices in oxygen and moisturefree atmospheres become more sophisticated and accessible, it is also necessary to focus on fundamental and systemindependent photodegradation pathways that occur under oxygen-free environments. Understanding these photodegradation pathways will allow researchers to gain a deeper understanding of the structure-property relationships impacting photostability.

Studies on P3HT have provided a foundational understanding of the role of common structural motifs in photodegradation both in the presence and absence of oxygen, where prevalent degradation pathways are shown in Figure S1.

In the solid state, the primary site where photodegradation readily begins occurs through the hexyl side chains, which are ubiquitously used as solubilizing groups in conjugated polymers. In particular, the C-H bond on the benzylic-like CH<sub>2</sub> attached directly to the conjugated backbone is particularly prone to homolytic cleavage, as the radical formed can be stabilized through delocalization into the thiophene ring. This then cascades into many complex degradation pathways that depend on the presence of oxygen or lack thereof, such as fragmentation of the alkyl chains as well as ketone or alcohol formation. <sup>4,18–20</sup> Trace metal impurities in the polymer, such as iron from an oxidative polymerization or impurities introduced during monomer synthesis, were implicated in initiating radical formation at the CH2 sites, highlighting the importance of rigorous purification and a possible reason for lab-to-lab/batch-to-batch reproducibility issues. 1,11 Additionally, while chain scission has mainly been observed in the presence of oxygen, crosslinking can occur even in the absence of oxygen. Both processes proceed, in P3HT at least, through a free-radical mechanism that is not initiated by oxygen, but rather through trace metal impurities as described above. 11,13,21-23 Finally, under ambient conditions, oxidation of the thiophene sulfur is also observed. Despite all of these possible degradation pathways, P3HT nevertheless remains one of the most photostable conjugated polymers. In a study that rigorously excluded oxygen, P3HT displayed a negligible drop in absorbance after 1000 h of irradiation in a SEPAP 12/24 unit using mercury lamps, and a 20% loss in absorbance over 10,000 h of irradiation. While impressive and encouraging, this clearly shows photodegradation continues to occur, and at a rate that is problematic for applications requiring years of photostability. This again highlights the importance of studying the photodegradation mechanisms that continue to persist even in the absence of oxygen, and to devise strategies and structural design rules that suppress these pathways.

Here, we report on how the choice of side chain branching and placement impacts solid-state photostability by studying a family of dialkoxy-functionalized thiophene polymer thin films irradiated under AM 1.0 at 1 sun irradiance level in an inert atmosphere. Importantly, through a combination of UV—vis absorbance spectroscopy that quantifies the photostability of the chromophore, X-ray photoelectron spectroscopy (XPS) that provides information about chemical changes occurring during irradiation, and size exclusion chromatography (SEC) that can elucidate the role of chain scission and crosslinking, we gain a more complete picture of photodegradation in the studied materials and propose design rules that are straightforward to adopt and should lead to enhanced

photostability. We have chosen building blocks that have been extensively studied for use in organic electronics and also allow for straightforward modulation of side chain properties in terms of placement, design, and branching points. Finally, we investigate the electrochemical performance of irradiated films to gain a complete picture of how photodegradation impacts material properties. Importantly, we show how crosslinking compromises electroactivity to an extent not readily evident from other results. From these findings, we believe that moving away from tertiary carbon branched side chains toward either quaternary carbon branches or linear chains and/or moving the branching point further from the conjugated backbone will all be strategies to enhance the photostability of conjugated polymers.

#### **■** EXPERIMENTAL SECTION

**Materials.** The repeat unit structures for the studied polymers are shown in Figure 1. P3HT was purchased from Rieke Metals [4002-E; rr > 90%; manufacturer specifications =  $M_{\rm W}$  50–70k; measured  $M_{\rm n}$  = 21.8 kg/mol, D = 2.3]. All other polymers—3,3-bis(2-ethylhexyloxymethyl)-3,4-dihydro-2H-thieno[3,4-D][1,4]dioxepine (P(ProDOT)-B),  $M_{\rm n}$  = 11.4 kg/mol, D = 1.6), $^{2+}$  3,4-bis((2-ethylhexyl)oxy)thiophene (P(DOT)-B),  $M_{\rm n}$  = 56 kg/mol, D = 5.4), $^{25,26}$  3,4-bis(hexyloxy)thiophene (P(DOT)-L),  $M_{\rm n}$  = 15 kg/mol, D = 2.2), $^{27}$  and 3,3-bis(((2-ethylhexyl)oxy)methyl)-6-(3,3',4,4'-tetrakis((2-ethylhexyl)oxy)-[2,2'-bithiophen]-5-yl)-3,4-dihydro-2H-thieno[3,4-D][1,4]dioxepine (P(DOT)-B-D-D0-D0, D0, D0, D1.8 kg/mol, D1.8 kg/mol, D2.2),D6—were synthesized using previously reported conditions. P(DOT)-B was synthesized using oxidative polymerization, while all other polymers were synthesized using direct arylation polymerization. GPC traces of all polymers are reported in Figure 5 and Figure S8. Full characterization (NMR, elemental analysis, etc.) can be found in the citations for each polymer.

To prepare the films, P(DOT)-B, P(ProDOT)-B-co-(DOT)-B, and P(ProDOT)-B were dissolved in toluene; P3HT and P(DOT)-L were dissolved in CHCl<sub>3</sub>. For spray-coated films, 4-5 mg/mL solutions were prepared and stirred overnight. Films were sprayed using an Iwata-Eclipse HP-BS spray gun, using 20 psi nitrogen or argon as the carrier gas, while maintaining an approximate distance of ca. 10-15 cm from the substrate. All sprayed films were cast to an optical density of 1.0  $\pm$  0.1. It has been shown that in order to compare the photostability of different films, materials should be coated to comparable absorbances. <sup>14</sup> For most samples tested, different polymers were sprayed side by side and encapsulated on the same glass slide to ensure that irradiation results occurred in the same encapsulated environment. For drop-casting, 20-30 mg/mL polymer solutions were prepared and stirred overnight. Films were then prepared by depositing 5 mg on glass microscope slides in 100  $\mu$ L aliquots using a micropipette. Afterward, a film was also spray-coated on the same slide next to the drop-cast film to an optical density between 0.5 and 1; the absorption spectrum of the sprayed film could then be monitored to verify how well the cell was encapsulated since the drop-cast film is too thick to easily monitor using spectroscopic techniques. Films that were evaluated using X-ray photoelectron spectroscopy (XPS) were spray-coated onto glass slides, whereas films that were evaluated using size-exclusion chromatography (SEC) or nuclear magnetic resonance (NMR) were drop-cast on glass to obtain enough material (ca. 5 mg) for analysis. Finally, films that were evaluated electrochemically were spray-coated on ITO/glass (Delta Technologies, 8-12 ohm/sq) and tested in an electrolyte solution consisting of 0.1 M tetrabutylammonium hexafluorophosphate (TBAPF6, purified by recrystallization from hot ethanol) dissolved in propylene carbonate (PC), using a Pt flag as a counter electrode and a Ag/AgCl as the reference electrode (calibrated vs Fc/Fc $^+$ ,  $E_{1/2}$  = 0.40V). SEC of all polymers was measured in CHCl<sub>3</sub> vs polystyrene at 40 °C.

**Sample Encapsulation.** A schematic of the encapsulated cell and accompanying photographs are shown in Figure S2. After coating, the

films were placed under vacuum ( $10^{-3}$  Torr) for at least 1 h before bringing them into a glovebox ( $O_2 < 50$  ppm;  $H_2O = 0.5$  ppm). A 0.5 mm-thick ADCO polyisobutylene edge sealant gasket, at least 2 mm wide, was applied around the edge of the substrate and a glass microscope slide placed on top to seal the film. ADCO strips should be placed so that each one is flush against the other and without overlapping one another. To activate the sealant, the cell was placed on a hotplate ( $100-110~^{\circ}\text{C}$ ) for ca. 1-2 min followed by pressing the cell firmly between the fingertips. The sealant noticeably deformed, and minimal air bubbles should be observed between the sealant and the glass. The cell was turned over and placed back on the hotplate and the heating/pressing procedure repeated two more times to ensure good encapsulation. The procedure and conditions were designed to be reproducibly and rigorously sealed to allow accurate comparisons of samples to be made.

Sample Testing. Cells were irradiated using an Atlas XLS+ Suntest solar simulator, equipped with a 1700 W xenon arc lamp and a daylight filter operating at 1000 W/m<sup>2</sup> (55 W/m<sup>2</sup> between 300 and 400 nm). The temperature inside the chamber was 35  $^{\circ}\text{C}$  as measured at the chamber floor by a thermocouple, and 55 °C at a black standard temperature sensor throughout the test. The cells were taken out periodically to measure their absorbance spectra using an Ocean Optics USB 2000+ spectrophotometer. For all optical measurements, the spectra were blanked vs a cell consisting of either glass/ADCO/ glass or glass/ADCO/ITO/glass. After irradiation, cells were disassembled and the films were evaluated by cyclic voltammetry and XPS. Samples for SEC and NMR were prepared by immersing the films in a vial containing the appropriate solvent (chloroform and CDCl<sub>3</sub> for SEC and NMR, respectively) for dissolving the polymer samples prior to further analysis. More details on the experimental conditions and instrumentation can be found in the Supporting Information.

#### ■ RESULTS AND DISCUSSION

#### Structural Considerations for Photostable Materials.

The family of dioxythiophene polymers evaluated in this study, shown in Figure 1, was selected with two key structural motifs in mind: the first was to examine structures with oxygen atoms adjacent to the conjugated backbone, and the second was to study a family of materials with different degrees of twisting along the backbone. As the main photodegradation pathway in P3HT starts with H-abstraction at the  $\alpha$ -carbon on the alkyl side chains, strategies to improve photostability have focused on eliminating this weak point altogether, such as by designing polymers with thermally cleavable side chains, or electro-polymerizing subunits with no side chains. 11,14,28,29 A less explored approach is to use alkoxy instead of alkyl side chains, as attaching an oxygen to the aromatic ring can prevent radicals formed on the alkyl chain from delocalizing into the conjugated backbone. 9,10,20,30,31 Furthermore, the bond dissociation energy of the Ca-H bond in an alkoxy chain (i.e., the carbon adjacent the oxygen) is 7-8 kcal/mol higher than that of the  $C_{\alpha}$ -H bond in an alkyl chain (i.e., the carbon adjacent the aromatic ring), making the homolytic cleavage along alkoxy chains less energetically favorable.<sup>30</sup>

Regarding the second design motif, a previous survey of oligomers and polymers observed that materials with larger dihedral angles along the conjugated backbone were notably less photostable than their planar analogs.<sup>3,4,17,32</sup> To probe the relationship between the dihedral angle and photostability further, all the polymers in this study possess the same dioxythiophene core, but the degree of backbone twisting is tuned through the choice of side chains. This allows the trend in dihedral angles to be inferred from the optical properties of the polymers, where the more twisted systems would have the most blue-shifted absorbance spectra and the more planar

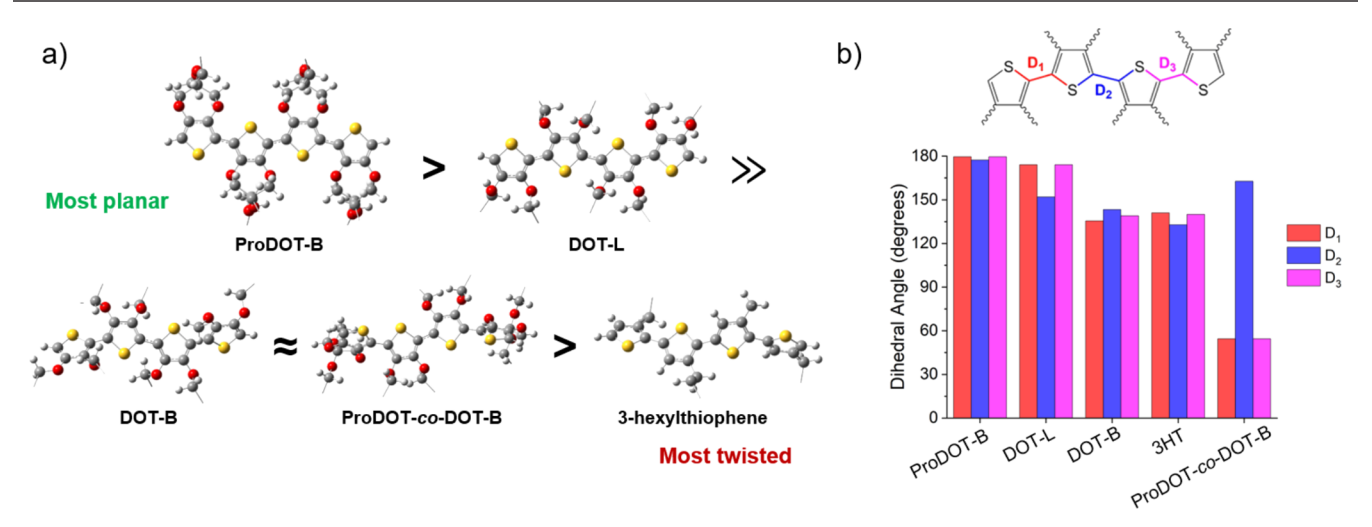


Figure 2. (a) Gas-phase DFT-derived ball-and-stick structures of the four-ring model compounds representing the polymers in this study. (b) Dihedral angles between each of the rings.

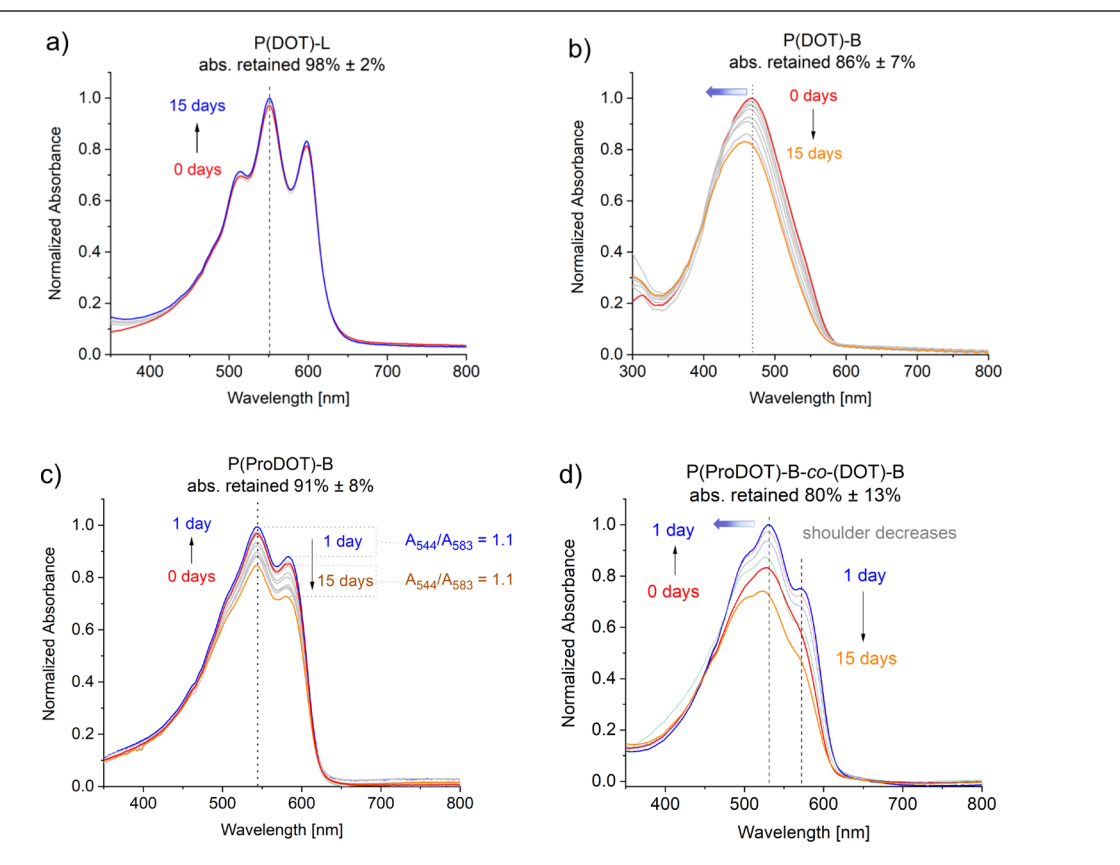


Figure 3. Evolution of absorbance over 15 days of irradiation for the family of polymers outlined in Figure 1: (a) P(DOT)-L, (b) P(DOT)-B, (c) P(ProDOT)-B, and (d) P(ProDOT)-B-co-(DOT)-B. At least five samples of each polymer were spray-coated to 1.0  $\pm$  0.1 au on glass, encapsulated, and irradiated; a representative absorbance spectrum for each polymer is shown here. The dashed line serves as a visual guide for how the peak position evolves during irradiation.

systems would have the most red-shifted spectra. We further confirmed this trend using gas-phase DFT calculations on oligomers consisting of four monomer units (Figure 2 and Figures S3 and S4). From these calculations, we find that the DOT-L oligomer containing linear side chains has a notably smaller degree of twisting (avg. 167°, where 180° is the planar structure with the S atoms of the thiophene rings anti to one another) than its branched analog DOT-B (avg. 139°). Ball-and-stick models in Figure 2 and Figure S4 show that in spite of the size of the linear alkyl chain, they are able to extend

outward without inducing significant torsional strain. Interestingly, moving the branched side chain further from the conjugated backbone and placing it on an sp³ hybridized carbon lead to a highly planar ProDOT-B oligomer (avg. 179°), where the branching point can extend out of the plane of the backbone to minimize its disruption on backbone planarity. The ProDOT-DOT-DOT-ProDOT oligomer, which models the behavior of the copolymer, appears dominated by the DOT-B subunit, giving rise to large dihedral angles and a loss of anti-orientation of the thiophenes. These trends are

relatively well reflected in the absorption spectra of the polymer thin films in Figure 3. Notably, the spectra of P(DOT)-L and P(ProDOT)-B are similar both in terms of the onset of absorption and  $\lambda_{\rm max}$  suggesting that the polymers have a comparable degree of planarity in the solid state. Similarly, the copolymer's onset of absorption and  $\lambda_{\rm max}$  are in between those of P(DOT)-B and both P(DOT)-L and P(ProDOT)-B, also suggesting that some degree of planarization is induced in the solid state.

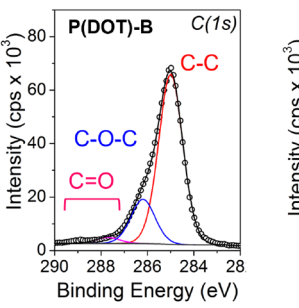
Probing Spectral Changes vs Irradiation Time. Monitoring the change in absorbance as a function of irradiation time is a widespread approach for assessing the photostability of conjugated polymers where a loss in the  $\pi - \pi^*$  absorption is often associated with the degradation of the chromophore. While UV-Vis-NIR spectroscopy does not provide insights into degradation pathways, or even serve as a predictor for how film performance is impacted, it is heavily relied upon for evaluating photodegradation and it is valuable as a straightforward first approximation of photodegradation. In Figure 3, we show the UV-vis-NIR spectra of polymers encapsulated between glass slides under an inert atmosphere and demonstrate how the absorption profile changes during 15 days of "accelerated testing" (i.e., 15 days in the irradiation chamber corresponds to 15 weeks of outdoor Florida Sun). Over these 15 days, we observed a 91%  $\pm$  6% retention of the  $\pi - \pi^*$  absorption in P3HT (used here as a control polymer) and no shifting in the absorption maximum or in the absorption peak ratios (Figure S5). Among the dioxythiophene systems studied here, the polymer that displayed the least change under these irradiation conditions is the n-octyl functionalized P(DOT)-L, which retains nearly all its absorbance (98% ± 2%, Figure 3a) throughout the duration of the experiments. In contrast, when branching points are introduced in the alkyl side chains, P(DOT)-B displays a more rapid loss of the  $\pi - \pi^*$  absorption (86% ± 11% retained, Figure 3b) in addition to a hypsochromic shift, suggesting that the branched carbon motif is more susceptible to photodegradation. Moving the side chains away from the backbone but maintaining the branching point resulted in a small enhancement of the average absorption retention with P(ProDOT)-B performing comparably to P3HT, retaining 91%  $\pm$  8% of its initial absorbance without undergoing a blueshift or affecting the peak ratios (Figure 3c). Finally, the copolymer (P(ProDOT)-B-co-(DOT)-B) containing branched dialkoxythiophene units on both units again displays not only a loss of absorbance (80%  $\pm$  13% retained) but also a hypsochromic shift and a loss of a long-wavelength shoulder (Figure 3d). This gives further support to the idea that branched alkyl chains are linked to increased rates of photodegradation. Furthermore, in DOT-B-containing polymers with alkyl branching points near the conjugated backbone, the spectral blue-shift and decrease in longwavelength absorption during photodegradation suggest that a change in the effective conjugation length occurs over the course of irradiation, either due to changes in intermolecular interactions, twisting along the backbone, or chain scission. As will be discussed later, our results suggest that the spectral changes observed in polymers with branching points close to the backbone are due to increased twisting induced by polymer crosslinking. In contrast, polymers with linear side chains or with side chains not directly adjacent to the backbone show a uniform loss in absorbance that maintains the same absorbance

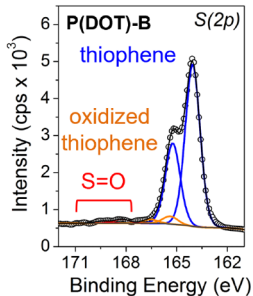
profile, indicating minimal conformational changes during irradiation.

Probing Functional Group Formation and Fragmentation via XPS. While not as widely used as absorption spectroscopy or FTIR in irradiation studies, XPS provides quantitative information regarding the ratios and chemical state of elements on the surface of the films. In the scope of the degradation mechanisms shown in Figure S1, this would allow us to evaluate whether the fragmentation of side chains occurs as we would observe a change in the ratio of elements, such as carbon to sulfur atoms. While formation of carbonyls or oxygen attack at the thiophene sulfur is not expected given the ppm levels of oxygen present during the construction of our cells, unanticipated pathways for rearrangement may exist via the oxygen attached to the heterocycle. Additionally, by verifying the lack of carbonyl or sulfonyl formation, XPS confirms that external sources of oxygen remained excluded throughout the experiment.

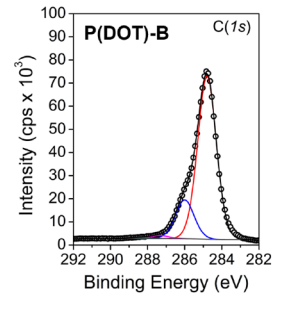
In Figure 4, we show an example of the XPS signals arising from the carbon and sulfur peaks for P(DOT)-B before and

#### unirradiated





#### 15 days irradiation



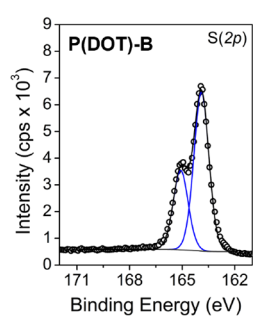


**Figure 4.** XPS of P(DOT)-B showing the core level spectra of C(1s) and S(2p) from an unirradiated film and a film irradiated for 15 days. These films do not display any of the signature increases from carbonyl or sulfone groups.

after irradiation to determine whether the changes observed in the absorbance spectrum in Figure 3b are correlated with any changes in chemical composition. In the unirradiated sample, the carbon signal is composed primarily of peaks arising from carbon—carbon bonds (284.8 eV) and carbon—oxygen bonds (286.5 eV) as well as trace amounts of oxidized carbon peaks (C=O, 288 eV and O-C=O, 289 eV) from adventitious carbon, a thin layer of carbonaceous material arising from exposure of films to the atmosphere. The sulfur peak shows a doublet pattern arising from the  $S(2p_{1/2})$  and  $S(2p_{3/2})$  characteristic of the thiophene sulfur (165 eV). The binding

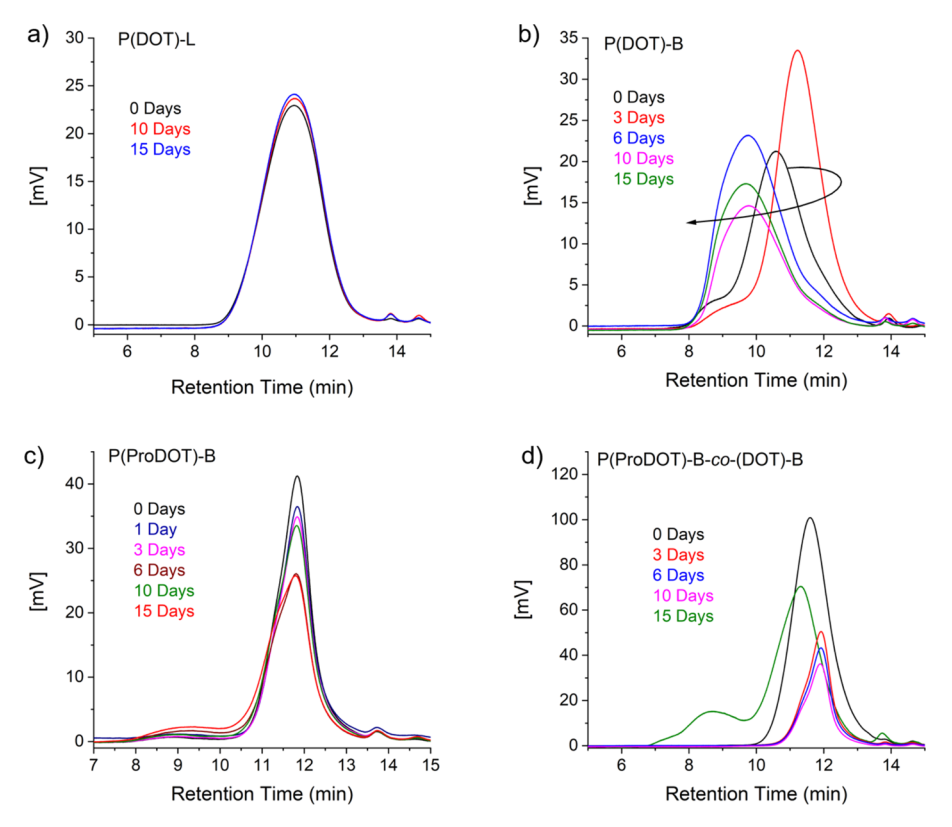


Figure 5. SEC traces of (a) P(DOT)-L, (b) P(DOT)-B, (c) P(ProDOT)-B, and (d) P(ProDOT)-B-co-(DOT)-B over 15 days of irradiation.

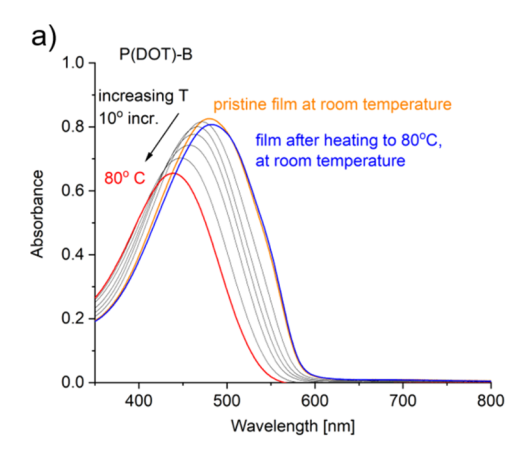
energies where we would expect to observe signs of attack by oxygen are marked, specifically carbonyl formation (288–289 eV) and sulfur oxygen double bond formation (168 eV). After 15 days of irradiation, we did not observe any signals at these binding energies, indicating that these side products were not being formed to any appreciable extent at the surface in any of the films. Additionally, the elemental ratios remained nearly the same before and after irradiation. This not only confirms that our encapsulation process was rigorous, but also rules out the presence of any side chain fragmentation or loss of sulfur. Rearrangements involving the oxygens attached to the heterocycle were not observed and can also be ruled out. Importantly, these trends were observed in all polymers studied (Figure S6, Supporting Information).

Probing Crosslinking through the Alkyl Side Chains Using Size-Exclusion Chromatography and NMR. From the XPS results, it is clear that reactions that either change the chemical state, such as reactions involving oxygen, or change the ratio of elements, such as side chain fragmentation, are not occurring in the encapsulated films, and these mechanisms cannot be invoked to explain the loss, and in some cases blueshifting, of the  $\pi$ - $\pi$ \* absorption. We next investigate whether crosslinking or chain scission is occurring upon irradiation, as these are reactions that would be difficult, if not impossible, to detect via XPS. In order to observe these processes, sizeexclusion chromatography (SEC) was used to measure retention times and provide qualitative information of the changes in the hydrodynamic volume of pristine/unirradiated polymers and samples irradiated under an inert atmosphere for different amounts of time. If crosslinking were occurring, the polymer hydrodynamic volume would increase and lead to samples eluting faster and having a shorter retention time.

Alternatively, if samples were undergoing chain scission, longer retention times would be expected.

Figure 5 shows how the elution pattern of the polymers evolves over 15 days of irradiation. Importantly, all polymers with branched chains-most notably P(DOT)-B as well as P(ProDOT)-B-co-(DOT)-B and to a small extent P-(ProDOT)-B-all show the growth of a signal at lower retention times, indicating a higher molecular weight component being formed, which suggests that crosslinking is indeed occurring. Qualitatively, we also observed (Figure S7) that samples containing the branched dialkoxythiophene (P(DOT)-B and P(ProDOT)-B-co-(DOT)-B) as well as P(ProDOT)-B irradiated beyond 15 days were no longer fully soluble in toluene or chloroform, while unirradiated samples readily dissolved at concentrations greater than 50 mg/mL. P(DOT)-B displays the most complex degradation pathway, where the retention time increased after brief irradiation but then decreased, suggesting that both chain scission and crosslinking ocurred. A similar combination of both processes had previously been observed for P3HT irradiated in a chloroform solution to support this interpretation. 11 In contrast, both P3HT (Figure S8) and P(DOT)-L bearing linear side chains showed no changes in retention time through half a month of irradiation, and also remained fully soluble in chloroform, giving further support to the absence of crosslinking in these polymers.

As a final technique to understand the degradation pathway, <sup>1</sup>H NMR was performed on the polymer with the poorest photostability, P(ProDOT)-B-co-(DOT)-B (Figure S9). As the changes were expected to be subtle, the most photodegraded polymer would best magnify any peak evolution that occurred during photodegradation. Two important trends stood out: first, small changes to relative peak intensities as well as new



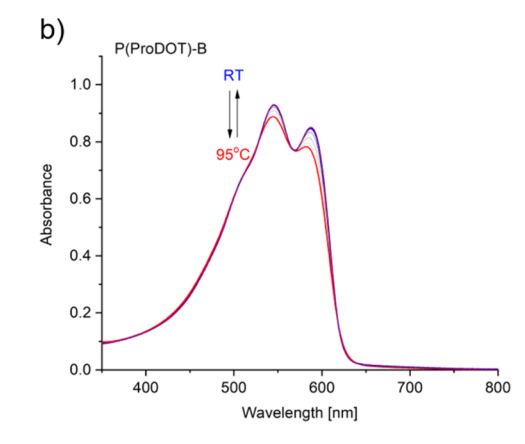


Figure 6. UV—vis spectra of (a) P(DOT)-B and (b) P(ProDOT)-B films on ITO/glass immersed in propylene carbonate as a function of applied temperature following a heat—cool protocol from room temperature to 80–95 °C and then back again to room temperature.

peaks were observed in the alkyl chain region of the spectrum (1.0 ppm <  $\delta$  < 1.2 ppm), consistent with the observed degradation arising from crosslinking through the alkyl side chains. Second, no changes were observed elsewhere, indicating that the conjugated backbone remains intact during photodegradation. From the combined XPS, SEC, and NMR results, we conclude that crosslinking through the alkyl side chains is the primary degradation pathway in oxygen-free photoirradiation of dialkoxythiophene polymers, with branched chains being particularly susceptible, especially as the branching point moves closer to the conjugated backbone.

Crosslinking as a Fundamental Oxygen-Free Photodegradation Pathway. The findings above raise the following questions: what fundamental oxygen-free photodegradation pathways are consistent with the observed results, and what structural modifications could suppress these pathways? How do we explain the change in the absorption profile if the chromophore itself is not compromised? Finally, what are the consequences of photodegradation on physical properties? From the mechanisms outlined in Figure S1, we see that C-H heterolytic bond cleavage occurs in the absence of oxygen; this radical in turn is capable of reacting with neighboring chains, especially when branching points are present, resulting in the crosslinking that we have demonstrated in these polymers. This points to fundamental degradation pathways that could not be suppressed even through the use of improved oxygen/moisture barrier layers. These results do suggest, however, that replacing branched chains with linear chains is a promising strategy for improved photostability. It may also be possible to use a quaternary branched groups if branching is needed to induce solubility, as this would also lead to a functionality without a tertiary hydrogen. Additionally, moving the branching point further from the conjugated backbone may also reduce the impact of crosslinking on the backbone conformation. Finally, we note that when dialkoxy side chains are utilized as solubilizing chains, no propagation of radicals from side chains into the heterocycle are observed, which strongly supports the use of this side chain motif.

Absorbance Changes Arising from Crosslinking and Ring Twisting. While the changes in absorbance over prolonged irradiation serve as the first indication that some form of degradation is occurring, how does crosslinking explain the changes we see, specifically a loss in absorbance and a blueshifting of the spectra? In the literature, while the mechanism

of degradation during photoirradiation has been the subject of much investigation for P3HT, the loss in absorbance in conjugated polymers has not been as well-understood. A few explanations have been proposed but are not consistent with the results in this study. For example, pathways involving loss of conjugation via ring opening or formation of electron-withdrawing functional groups have involved oxygen, which is not present in our systems, nor are the chemical signatures of these pathways observed. A loss in film thickness has also been shown to occur in previous studies; however, this coincided with the fragmentation of side chains, which we again do not observe here. 18,19

We propose that crosslinking leads to increased twisting between rings in systems where the branching point is close to the backbone (namely, P(ProDOT)-B-co-(DOT)-B and P-(DOT)-B), which directly leads to a blue-shifting of the spectra due to the disruption of conjugation and thus a loss in optical density. Crosslinking at branching points further from the backbone (as with P(ProDOT)-B) is far less disruptive. A previous study on chemically crosslinked conjugated polymers also noted that crosslinking close to the backbone leads to distortions in conjugation and, by extension, a blue shifting of the absorbance spectrum while crosslinking further from the backbone leads to minimal disruption.<sup>33</sup> To demonstrate that changes to polymer chain organization alone can impact thin film absorbance, thermochromism of a P(DOT)-B film was evaluated, as shown in Figure 6a, where we see that the film can reversibly undergo similar changes to those observed during irradiation solely as a function of temperature. As we heat the sample from room temperature to 80 °C, the spectrum not only loses intensity but also blue-shifts. In general, these spectral trends point to an increased conformational disorder, through a combination of ring-twisting, which blue-shifts, broadens, and decreases the intensity of the absorbance, and deaggregation, which also would give rise to a blue-shifted spectrum. Upon cooling, the original spectrum and chain conformation are recovered. Demonstrating reversibility is important as it allows us to attribute these trends to reversible changes in conformation and not to irreversible chemical side reactions. In the irradiated films however, these conformational changes are made permanent by the crosslinks locking chains into more twisted conformations.

In contrast, when the side chains are moved further away from the backbone (e.g., P(ProDOT)-B, Figure 3c), a decrease

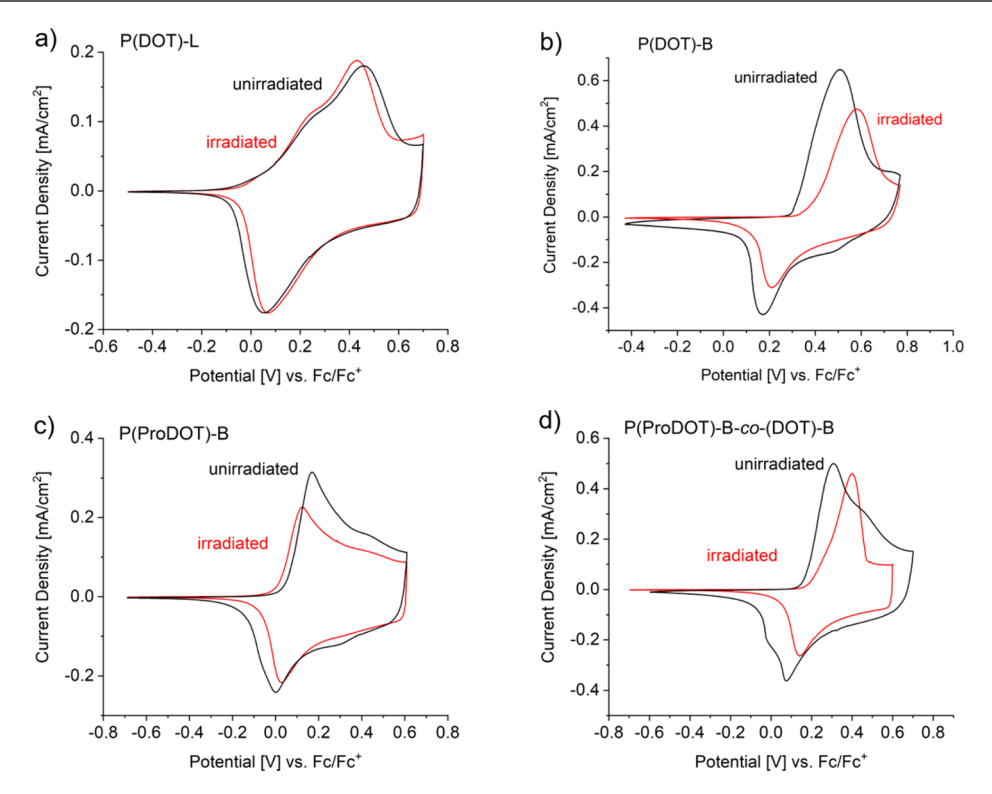


Figure 7. Cyclic voltammograms of (a) P(DOT)-L, (b) P(DOT)-B, (c) P(ProDOT)-B, and (d) P(ProDOT)-B-co-(DOT)-B before and after 15 days of irradiation.

in absorbance was observed during irradiation without any corresponding spectral blue-shift. Building on what was discussed in the previous paragraph, this behavior would suggest that subtle conformational changes, locked into place via a small amount of crosslinking as shown in Figure 5c, are occurring without chemical degradation of the conjugated backbone during irradiation. This is supported by the temperature-dependent absorbance in Figure 6b where we can induce a small and reversible loss in intensity due to increases in film disorder upon heating but not enough disorder to induce spectral blue-shifting. This demonstrates that when the side chains are not directly adjacent to the backbone, the polymer chain is less likely to undergo large conformational changes and also supports the idea that moving the branching point and inducing crosslinking further from the backbone help to minimize conformational changes to the conjugated backbone.

Finally, thermochromism of the copolymer containing both DOT and ProDOT subunits (P(ProDOT)-B-co-(DOT)-B, Figure S10) showed nearly identical trends to P(DOT)-B, where a notable decrease in absorbance intensity occurs upon heating followed by a blue-shift in the peak. Upon cooling, the original spectrum is once again re-obtained. This demonstrates that the thermochromic properties of the copolymer are dominated by the DOT-B subunit, which continues to induce large conformational changes in spite of the presence of the ProDOT subunit.

#### Impact of Photodegradation on Redox Properties.

We have shown how side chain engineering impacts optical and conformational properties of the conjugated backbone. However, changes to the polymer absorbance do not tell the full story of photodegradation, a relationship that is often implied in many studies. We emphasize the need to look further toward the impact of irradiation on the properties

relevant to the specific applications these materials are intended for. DOTs and ProDOTs have been extensively explored as redox-active materials, and by analyzing the cyclic voltammograms (CVs), we can elucidate what impact crosslinking through the side chains has on the redox properties. During electrochemical doping, electron transfer is initiated by biasing the underlying electrode and occurs at the polymer/electrode interface. At the same time, counter ion transport is required for charge neutrality as solvents and electrolytes move in and out of the polymer film. Upon oxidation, a geometric reorganization of the polymer chain must occur to accommodate the charge carriers, and some degree of swelling is necessary to accommodate charge balancing ions and solvents. In most cases, ion transport is regarded as the rate-limiting step during the doping process. The number of redox peaks observed varies from one polymer to another and is often attributed to the heterogeneous nature of polymer films where domains with different extents of interand intramolecular coupling give rise to electrochemically resolvable populations of chromophores.<sup>34–37</sup>

If the steric interactions induced by crosslinking increase backbone twisting, this would reduce the degree of the  $\pi$ -orbital overlap between repeat units, leading to an increase in the oxidation potential. In addition, shifts in peak positions can be indicative of hindered charge transfer between the polymer and the electrode, or by counter ion transport limitations through the film, both of which can be expected to be affected by crosslinking. By integrating the CV, we can extract the film's charge capacity, which is composed primarily of Faradaic current (i.e., current arising from the electron transfer process) and also a non-negligible amount of capacitive charging. A loss in charge capacity is often attributed to the degradation of the polymer backbone but can also be observed if electrolyte uptake or electron transfer is severely compromised and

provides a quantitative measure to compare the films' redox activity before and after irradiation.

Figure 7 highlights the effect of irradiation and crosslinking on the redox behavior of the polymers studied. As expected, P(DOT)-L, which showed no signs of photodegradation by any technique, exhibits negligible differences in the redox response in terms of the onset of oxidation, peak positions, relative peak current, and charge capacity after 15 days of irradiation (Figure 7a). In contrast, CVs of irradiated P(DOT)-B (Figure 7b) contain notable differences compared to the unirradiated films. We observe a shift in the onset of oxidation and in the oxidation peak to higher potentials. This supports the understanding that crosslinks formed induce backbone twisting, as we discussed in conjunction with Figures 3b and 6a, making the polymer more difficult to oxidize. We also observe a 33% loss in the charge capacity after irradiation. This is a greater loss in performance than would be expected from the optical changes observed during irradiation (i.e., ca. 14% decrease in absorbance and a slight blue-shift) and indicates that the impact of photoinduced crosslinking is not uniform across different material properties. Because our previous data shows that irradiation is not degrading the conjugated backbone, we believe that the decreased charge capacity is due to charge transfer and/or ion transport being negatively impacted by crosslinking, which in turn hinders the ability to access electroactive sites in irradiated films. The redox response of P(ProDOT)-B-co-(DOT)-B (Figure S11) closely resembles that of P(DOT)-B, which is not surprising given the similarities in their structure and changes observed in their optical properties as a result of photodegradation (blueshift and loss of intensity).

Turning to P(ProDOT)-B, we observe a smaller loss of 19% in charge capacity after irradiation, as shown in Figure 7c, which is more in line with the optical changes that we observed. This is also consistent with the smaller amount of crosslinking in P(ProDOT)-B (as shown in Figure 5) as well as having crosslinking sites located further away from the conjugated backbone, both of which would not significantly hamper ion transport through the film. Finally, we note that the onset of oxidation is nearly unchanged after irradiation and supports our understanding that no significant conformational changes have occurred.

These results first and foremost affirm our observation that linear alkoxy chains appended onto polythiophenes afford robust photostability both in terms of chemical stability and in retaining the polymer's electrooptical properties. Furthermore, it supports the motivation to move branched side chains further from the conjugated backbone in order to decouple the changes happening at the side chains from impacting the dioxythiophene core and conjugated backbone. Finally, these results demonstrate how photoinduced crosslinking can have a more profound impact on some properties, (such as charge capacity) than others (such as optical properties), necessitating a thorough evaluation of materials' properties to gain a complete picture of how photoirradiation affects not just the chemical structure, but also how the polymer interacts with its environment.

#### CONCLUSIONS

Photoirradiation with AM 1.0 light under an inert atmosphere of a family of dioxythiophene polymers has shed light on the role of various structural motifs in photodegradation. Under proper encapsulation and in the absence of oxygen, chemical

degradation of the conjugated backbone does not occur to any appreciable extent. The differences in the rate of photodegradation observed in the polymers studied here are instead dependent on differences in side chain design, with the following structure-property relationships established based on our results. First and foremost, linear chain alkoxy functionalized XDOTs exhibit no loss in performance during irradiation in the absence of oxygen. Second, mechanistically, hydrogen atom abstraction on the side chain followed by crosslinking is the fundamental degradation pathway occurring in the absence of oxygen. Third, alkoxy side chains have the potential to offer enhanced photostability superior to P3HT in the case of linear chains. Fourth, while branched alkoxy chains are more prone to photodegradation than linear chains, there are design possibilities that can reduce degradation rates, such as moving the branching point further from the conjugated backbone. We believe these results offer design guidelines applicable to the broader conjugated materials community, motivating the use of linear alkoxy side chains as well as minimizing the amount of tertiary hydrogen sites. Further probing of how branching point distance from the backbone impacts photostability will be necessary to optimize the design of branched substituents. In addition to informing design, it is equally important to note that demonstrating absorption loss during irradiation does not always result from chemical degradation of the conjugated backbone, but it can be accounted for by torsional strain locked into place by photoinduced crosslinking. Finally, we gain a complete picture of how the chemical and structural consequences of photodegradation impact film performance by evaluating the redox properties of our materials. In our study, changes in optical properties during photoirradiation only tell part of the story: photodegradation that only impacts the conjugated backbone through subtle changes in order and torsional strain, such as the photoinduced crosslinking occurring in the side chains of our systems, will have a small impact on optical properties. However, these changes play a larger role when evaluating and comparing the redox behavior of these polymers, as electrolyte flux in and out of the films (and the swelling/deswelling that accompanies that) is necessary for achieving reversible electrochemical doping. As we explore novel structures using the design motifs developed through this study, the experiments laid out here offer a roadmap for holistically evaluating their performance and suitability for developing photostable electrochemical devices.

#### ASSOCIATED CONTENT

#### **Solution** Supporting Information

The Supporting Information is available free of charge at https://pubs.acs.org/doi/10.1021/acs.chemmater.1c03317.

Full experimental and instrument information, XPS, absorbance spectra, NMR, and CVs of all polymers (PDF)

#### AUTHOR INFORMATION

#### **Corresponding Authors**

D. Eric Shen — School of Chemistry and Biochemistry, School of Materials Science and Engineering, Center for Organic Photonics and Electronics, Georgia Tech Polymer Network, Georgia Institute of Technology, Atlanta, Georgia 30332, United States; orcid.org/0000-0002-8318-898X; Email: eric.shen@chemistry.gatech.edu

John R. Reynolds — School of Chemistry and Biochemistry, School of Materials Science and Engineering, Center for Organic Photonics and Electronics, Georgia Tech Polymer Network, Georgia Institute of Technology, Atlanta, Georgia 30332, United States; ⊙ orcid.org/0000-0002-7417-4869; Email: reynolds@chemistry.gatech.edu

#### **Authors**

- Augustus W. Lang School of Materials Science and Engineering, Center for Organic Photonics and Electronics, Georgia Tech Polymer Network, Georgia Institute of Technology, Atlanta, Georgia 30332, United States
- Graham S. Collier School of Chemistry and Biochemistry, School of Materials Science and Engineering, Center for Organic Photonics and Electronics, Georgia Tech Polymer Network, Georgia Institute of Technology, Atlanta, Georgia 30332, United States; Department of Chemistry and Biochemistry, Kennesaw State University, Kennesaw, Georgia 30144, United States; orcid.org/0000-0002-9650-8110
- Anna M. Österholm School of Chemistry and Biochemistry, School of Materials Science and Engineering, Center for Organic Photonics and Electronics, Georgia Tech Polymer Network, Georgia Institute of Technology, Atlanta, Georgia 30332, United States; orcid.org/0000-0001-6621-8238
- Evan M. Smith Department of Chemistry/Biochemistry, University of North Georgia, Dahlonega, Georgia 30597, United States
- Aimée L. Tomlinson Department of Chemistry/ Biochemistry, University of North Georgia, Dahlonega, Georgia 30597, United States

Complete contact information is available at: https://pubs.acs.org/10.1021/acs.chemmater.1c03317

#### **Author Contributions**

G.S.C. performed SEC and NMR, analyzed the data, and prepared figures. A.W.L. performed XPS, analyzed the data, and prepared XPS figures. D.E.S. performed all remaining experiments and wrote the manuscript. A.M.Ö. provided data analysis, especially regarding electrochemical results. E.M.S. and A.L.T. performed DFT calculations and prepared the corresponding figures. The manuscript was written through contributions of all authors. All authors have given approval to the final version of the manuscript.

#### Notes

The authors declare no competing financial interest.

#### ACKNOWLEDGMENTS

We thank the Office of Naval Research (N00014-20-1-2129 and N00014-20-1-2673) and Department of Energy (through the Bioenergy Engineered Products Synthesis Program EE0008494) for funding this work. SEC measurements were performed at the Organic Materials Characterization Laboratory (OMCL) at Georgia Tech; XPS was performed at the Georgia Tech Institute of Electronics and Nanotechnology, a member of the National Nanotechnology Coordinated Infrastructure, which is supported by the National Science Foundation (grant ECCS1542174).

#### REFERENCES

(1) Abdou, M. S. A.; Holdcroft, S. Photochemistry of Electronically Conducting Poly(3-Alkylthiophenes) Containing FeCl4- Counterions. *Chem. Mater.* **1994**, *6*, 962–968.

- (2) Manceau, M.; Chambon, S.; Rivaton, A.; Gardette, J.-L.; Guillerez, S.; Lematre, N. Effects of Long-Term UVvisible Light Irradiation in the Absence of Oxygen on P3HT and P3HT: PCBM Blend. Sol. Energy Mater. Sol. Cells 2010, 94, 1572—1577.
- (3) Hintz, H.; Egelhaaf, H. J.; Lüer, L.; Hauch, J.; Peisert, H.; Chassé, T. Photodegradation of P3HT A Systematic Study of Environmental Factors. *Chem. Mater.* **2011**, 23, 145–154.
- (4) Dupuis, A.; Wong-Wah-Chung, P.; Rivaton, A.; Gardette, J.-L. Influence of the Microstructure on the Photooxidative Degradation of Poly(3-Hexylthiophene). *Polym. Degrad. Stab.* **2012**, *97*, 366–374.
- (5) Bulloch, R. H.; Reynolds, J. R. Photostability in Dioxyheterocycle Electrochromic Polymers. J. Mater. Chem. C 2016, 4, 603–610.
- (6) Abdou, M. S. A.; Holdcroft, S. Solid-State Photochemistry of  $\pi$ -Conjugated Poly(3-Alkylthiophenes ). *Can. J. Chem.* **1995**, *1901*, 1893–1901.
- (7) Manceau, M.; Rivaton, A.; Gardette, J.-L.; Guillerez, S.; Lemaître, N. The Mechanism of Photo- and Thermooxidation of Poly(3-Hexylthiophene) (P3HT) Reconsidered. *Polym. Degrad. Stab.* **2009**, *94*, 898–907.
- (8) Perthué, A.; Fraga Domínguez, I.; Verstappen, P.; Maes, W.; Dautel, O. J.; Wantz, G.; Rivaton, A. An Efficient and Simple Tool for Assessing Singlet Oxygen Involvement in the Photo-Oxidation of Conjugated Materials. Sol. Energy Mater. Sol. Cells 2018, 2018, 336—339
- (9) Perthué, A.; Gorisse, T.; Santos Silva, H.; Bégué, D.; Rivaton, A.; Wantz, G. Influence of Traces of Oxidized Polymer on the Performances of Bulk Heterojunction Solar Cells. *Mater. Chem. Front.* **2019**, *3*, 1632–1641.
- (10) Sanow, L. P.; Sun, J.; Zhang, C. Photochemical Stability of Dicyano-Substituted Poly(Phenylenevinylenes) with Different Side Chains. *J. Polym. Sci., Part A: Polym. Chem.* **2015**, *53*, 2820–2828.
- (11) Abdou, M. S. A.; Holdcroft, S. Mechanisms of Photodegradation of Poly(3-Alkylthiophenes) in Solution. *Macromolecules* 1993, 26, 2954–2962.
- (12) Manceau, M.; Rivaton, A.; Gardette, J. L. Involvement of Singlet Oxygen in the Solid-State Photochemistry of P3HT. *Macromol. Rapid Commun.* **2008**, *29*, 1823–1827.
- (13) Caronna, T.; Forte, M.; Catellani, M.; Meille, S. V. Photodegradation and Photostabilization Studies of Poly(3-Butylthiophene) in the Solid State. *Chem. Mater.* **1997**, *9*, 991–995.
- (14) Tromholt, T.; Madsen, M. V.; Carlé, J. E.; Helgesen, M.; Krebs, F. C. Photochemical Stability of Conjugated Polymers, Electron Acceptors and Blends for Polymer Solar Cells Resolved in Terms of Film Thickness and Absorbance. J. Mater. Chem. 2012, 22, 7592–7601
- (15) Andrew, T. L.; Swager, T. M. Reduced Photobleaching of Conjugated Polymer Films through Small Molecule Additives. *Macromolecules* **2008**, *41*, 8306–8308.
- (16) Liang, Z.; Nardes, A.; Wang, D.; Berry, J. J.; Gregg, B. A. Defect Engineering in  $\pi$ -Conjugated Polymers. *Chem. Mater.* **2009**, 21, 4914–4919.
- (17) Mateker, W. R.; Heumueller, T.; Cheacharoen, R.; Sachs-Quintana, I. T.; McGehee, M. D.; Warnan, J.; Beaujuge, P. M.; Liu, X.; Bazan, G. C. Molecular Packing and Arrangement Govern the Photo-Oxidative Stability of Organic Photovoltaic Materials. *Chem. Mater.* **2015**, *27*, 6345–6353.
- (18) Domínguez, I. F.; Topham, P. D.; Bussière, P. O.; Bégué, D.; Rivaton, A. Unravelling the Photodegradation Mechanisms of a Low Bandgap Polymer by Combining Experimental and Modeling Approaches. J. Phys. Chem. C 2015, 119, 2166–2176.
- (19) Tournebize, A.; Bussière, P. O.; Wong-Wah-Chung, P.; Thérias, S.; Rivaton, A.; Gardette, J. L.; Beaupré, S.; Leclerc, M. Impact of Uv-Visible Light on the Morphological and Photochemical Behavior of a Low-Bandgap Poly(2,7-Carbazole) Derivative for Use in High-Performance Solar Cells. *Adv. Energy Mater.* **2013**, *3*, 478–487.
- (20) Tournebize, A.; Gardette, J. L.; Taviot-Guého, C.; Bégué, D.; Arnaud, M. A.; Dagron-Lartigau, C.; Medlej, H.; Hiorns, R. C.; Beaupré, S.; Leclerc, M.; Rivaton, A. Is There a Photostable

Conjugated Polymer for Efficient Solar Cells? *Polym. Degrad. Stab.* **2015**, *112*, 175–184.

- (21) Holdcroft, S. Photochain Scission of the Soluble Electronically Conducting Polymer: Poly(3-Hexylthiophene). *Macromolecules* **1991**, 24, 2119–2121.
- (22) Holdcroft, S. A Photochemical Study of Poly(3-Hexylthiophene). *Macromolecules* 1991, 24, 4834–4838.
- (23) Yamilova, O. R.; Martynov, I. V.; Brandvold, A. S.; Klimovich, I. V.; Balzer, A. H.; Akkuratov, A. V.; Kusnetsov, I. E.; Stingelin, N.; Troshin, P. A. What Is Killing Organic Photovoltaics: Light-Induced Crosslinking as a General Degradation Pathway of Organic Conjugated Molecules. *Adv. Energy Mater.* **2020**, *10*, 1903163.
- (24) Estrada, L. A.; Deininger, J. J.; Kamenov, G. D.; Reynolds, J. R. Direct (Hetero)Arylation Polymerization: An Effective Route to 3,4-Propylenedioxythiophene-Based Polymers with Low Residual Metal Content. *ACS Macro Lett.* **2013**, *2*, 869–873.
- (25) Dyer, A. L.; Craig, M. R.; Babiarz, J. E.; Kiyak, K.; Reynolds, J. R. Orange and Red to Transmissive Electrochromic Polymers Based on Electron-Rich Dioxythiophenes. *Macromolecules* **2010**, 43, 4460–4467
- (26) Kerszulis, J. A.; Johnson, K. E.; Kuepfert, M.; Khoshabo, D.; Dyer, A. L.; Reynolds, J. R. Tuning the Painter's Palette: Subtle Steric Effects on Spectra and Colour in Conjugated Electrochromic Polymers. J. Mater. Chem. C 2015, 3, 3211–3218.
- (27) Pittelli, S. L.; De Keersmaecker, M.; Ponder, J. F.; Österholm, A. M.; Ochieng, M. A.; Reynolds, J. R. Structural Effects on the Charge Transport Properties of Chemically and Electrochemically Doped Dioxythiophene Polymers. *J. Mater. Chem. C* **2020**, *8*, 683–693.
- (28) Manceau, M.; Helgesen, M.; Krebs, F. C. Thermo-Cleavable Polymers: Materials with Enhanced Photochemical Stability. *Polym. Degrad. Stab.* **2010**, *95*, 2666–2669.
- (29) Manceau, M.; Bundgaard, E.; Carlé, J. E.; Hagemann, O.; Helgesen, M.; Søndergaard, R.; Jørgensen, M.; Krebs, F. C. Photochemical Stability of  $\pi$ -Conjugated Polymers for Polymer Solar Cells: A Rule of Thumb. *J. Mater. Chem.* **2011**, 21, 4132–4141.
- (30) Silva, H. S.; Tournebize, A.; Bégué, D.; Peisert, H.; Chassé, T.; Gardette, J. L.; Therias, S.; Rivaton, A.; Hiorns, R. C. A Universal Route to Improving Conjugated Macromolecule Photostability. *RSC Adv.* **2014**, *4*, 54919–54923.
- (31) Kim, S.; Rashid, M. A. M.; Ko, T.; Ahn, K.; Shin, Y.; Nah, S.; Kim, M. H.; Kim, B. S.; Kwak, K.; Cho, M. New Insights into the Photodegradation Mechanism of the PTB7-Th Film: Photooxidation of  $\pi$ -Conjugated Backbone upon Sunlight Illumination. *J. Phys. Chem.* C **2020**, *124*, 2762–2770.
- (32) Luke, J.; Speller, E. M.; Wadsworth, A.; Wyatt, M. F.; Dimitrov, S.; Lee, H. K. H.; Li, Z.; Tsoi, W. C.; McCulloch, I.; Bagnis, D.; Durrant, J. R.; Kim, J. S. Twist and Degrade—Impact of Molecular Structure on the Photostability of Nonfullerene Acceptors and Their Photovoltaic Blends. *Adv. Energy Mater.* **2019**, *9*, 1803755.
- (33) Li, Y.; Zou, Y. Conjugated Polymer Photovoltaic Materials with Broad Absorption Band and High Charge Carrier Mobility. *Adv. Mater.* **2008**, 20, 2952–2958.
- (34) Skompska, M. Alternative Explanation of Asymmetry in Cyclic Voltammograms for Redox Reaction of Poly(3-Methylthiophene) Films in Acetonitrile Solutions. *Electrochim. Acta* **1998**, *44*, 357–362.
- (35) Skompska, M.; Szkurlat, A. The Influence of the Structural Defects and Microscopic Aggregation of Poly(3-Alkylthiophenes) on Electrochemical and Optical Properties of the Polymer Films: Discussion of an Origin of Redox Peaks in the Cyclic Voltammograms. *Electrochim. Acta* **2001**, *46*, 4007–4015.
- (36) Bruchlos, K.; Trefz, D.; Hamidi-Sakr, A.; Brinkmann, M.; Heinze, J.; Ruff, A.; Ludwigs, S. Poly(3-Hexylthiophene) Revisited Influence of Film Deposition on the Electrochemical Behaviour and Energy Levels. *Electrochim. Acta* **2018**, 269, 299–311.
- (37) Österholm, A. M.; Ponder, J. F., Jr.; De Keersmaecker, M.; Shen, D. E.; Reynolds, J. R. Disentangling Redox Properties and Capacitance in Solution-Processed Conjugated Polymers. *Chem. Mater.* **2019**, *31*, 2971–2982.

### **□** Recommended by ACS

Block Copolymer Stabilized Liquid Nanodroplets Facilitate Efficient Triplet Fusion-Based Photon Upconversion in Solid Polymer Matrices

Felipe Saenz, Christoph Weder, et al.

AUGUST 30, 2021

ACS APPLIED MATERIALS & INTERFACES

READ 🗹

## **Enhancement of Red Thermally Assisted Fluorescence in Bottlebrush Block Copolymers**

Alexander M. Polgar, Zachary M. Hudson, et al.

AUGUST 27, 2021

MACROMOLECULES

READ 🗹

#### Low-Band gap Conjugated Polymers with Strong Absorption in the Second Near-Infrared Region Based on Diketopyrrolopyrrole-Containing Quinoidal Units

Xuxia Zhao, Yanhou Geng, et al.

APRIL 04, 2021

MACROMOLECULES

READ **C** 

#### **Exploring Isomeric Effects on Optical and Electrochemical Properties of Red/Orange Electrochromic Polymers**

Graham S. Collier, John R. Reynolds, et al.

FEBRUARY 05, 2021

MACROMOLECULES

READ 🗹

Get More Suggestions >